Quantum limit of the contact resistance to low-dimensional materials

1st Emeric Deylgat
University of Texas at Dallas
IMEC
KU Leuven
Leuven, Belgium
emeric.deylgat@utdallas.edu

2nd Bart Sorée
IMEC
KU Leuven
Universiteit Antwerpen
Leuven, Belgium
bart.soree@imec.be

3rd William G. Vandenberghe
Departement of Materials Science and Engineering
University of Texas at Dallas
Dallas, Texas, USA
william.vandenberghe@utdallas.edu

***Abstract*—As device dimensions approach the nanoscale, contact resistance increasingly limits performance, particularly in low-dimensional systems where quantum mechanical effects dominate. In this work, we systematically investigate the quantum limit (QL) of contact resistance in 1D, 2D, and 3D semiconductors. Using general analytical expressions derived from ballistic transport theory and Fermi–Dirac statistics, we evaluate the QL across both the non-degenerate (Maxwell–Boltzmann) and degenerate (low-temperature) regimes. These expressions are validated against numerical simulations that incorporate electrostatic effects via the Poisson equation, allowing us to assess both fundamental and practical limits of contact resistance. Our results show that in the non-degenerate limit, all dimensionalities exhibit similar behavior, whereas in the degenerate limit, resistance increases exponentially as dimensionality decreases. When realistic contact electrostatics are included, the intrinsically weaker screening in lower-dimensional systems leads to more extended depletion regions, which influence resistance scaling in the non-degenerate regime. In contrast, in the degenerate limit, contact resistance is primarily governed by the quantum limit.**

***Index Terms*—Contact resistance, quantum limit, low-dimensional materials**

I. Introduction

Contact resistance is a major challenge in nanoscale devices, especially as shrinking dimensions bring quantum effects to the forefront. In low-dimensional systems, resistance is no longer governed by classical models but instead approaches a fundamental limit set by quantum transport principles [1], [2].This quantum limit (QL) arises from the discrete nature of conductance in confined systems and defines the lower bound for resistance under ballistic conditions.

Recent studies have shown that contacts in two-dimensional (2D) materials like MoS_2 can approach this limit. Through careful contact engineering that mitigates Fermi-level pinning and other detrimental mechanisms, contact resistances as low as 42 $\Omega\mu$m have been achieved [3]–[5]. However, inconsistent definitions of the QL in the literature have created confusion about what the correct mathematical formulation should be [6]. This highlights the need for a clear theoretical understanding of the QL across dimensions.

In this work, we analyze the QL of contact resistance in one-dimensional (1D), two-dimensional (2D), and three-dimensional (3D) semiconductor systems and examine the constraints imposed by dimensionality as devices scale to atomic thickness. We derive general analytical expressions for the QL in s-dimensional systems under both non-degenerate and degenerate carrier concentration limits, and validate them against numerical calculations. The analytical expression are then compared to numerical simulations of edge-contacted devices incorporating electrostatics, enabling analysis of the intrinsic QL in practical device configurations.

Figure 1 shows a schematic picture of the type of contacts considered in this paper. In (a), we show a conventional contact with a 3D semiconductor, where a bulk semiconductor is contacted by a metal. In (b), we show the 2D contact where a monolayer of a semiconductor makes a so-called edge-contact with a metal, preserving the dimensionality of the contact. Similarly, in (c) 1D semiconductor makes a contact with the metal only at the endpoint of the nano wire.

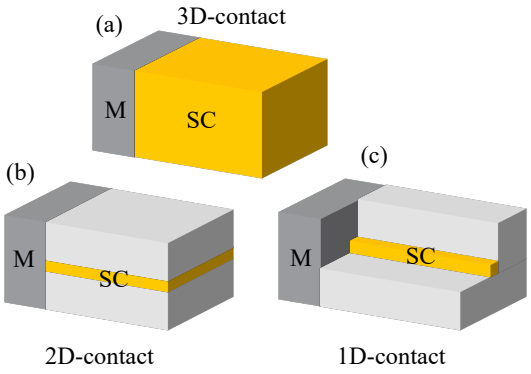

Fig. 1. Schematic illustration of the contact geometries considered in this work: (a) bulk contact, (b) monolayer edge contact, and (c) nanowire edge contact

II. Derivations & Methods

We determine the QL of contact resistance in a contact to an s-dimensional contact as

$$\frac{1}{R_{s\mathrm{D}}} = \frac{2e^2}{h} g_v \int dE \left| \frac{df(E)}{dE} \right| \int \frac{dk^{s-1}}{(2\pi)^{s-1}} T_{s\mathrm{D}}(\mathbf{k}, E) \quad (1)$$

where e is the elementary charge of the carriers, h is Planck's constant, g_v is the valley degeneracy of the conduction band,

$f(E)$ is the Fermi-Dirac distribution, and $T(\mathbf{k}, E)$ is the transmission of a particle at a certain wave vector $\mathbf{k}$ and total energy E. The integral over $\mathbf{k}$ goes over all the transverse direction perpendicular to the current direction. The transmission in a perfect ballistic material is given as

$$T_{s\mathrm{D}}(\mathbf{k}, E) = \begin{cases} 1 & \text{if } E > E_{\mathrm{C}} + (\Sigma_{i=0}^{s-1} \frac{\hbar^2 k_i^2}{2m^*}) \\ 0 & \text{else} \end{cases} \tag{2}$$

$$= \Theta\left(E - E_{\mathrm{C}} - \left(\Sigma_{i=0}^{s-1} \frac{\hbar^2 k_i^2}{2m^*}\right)\right) \tag{3}$$

where Θ is a step function, E_{C} is the conduction band energy level, m^* is the effective mass and the sum of the kinetic energies of the transverse directions i goes over all directions but not the current direction.

A. Carrier densities in s-dimensional materials

The carrier density in an s-dimensional semiconductor with a parabolic band is given by

$$n_{s\mathrm{D}} = \frac{2g_v}{(2\pi)^s} \int d^s k \, \frac{1}{1 + \exp\left(\frac{E(\mathbf{k}) - E_{\mathrm{F}}}{k_{\mathrm{B}} T}\right)}, \tag{4}$$

where $E(k) = \frac{\hbar^2 |\mathbf{k}|^2}{2m^*}$. This can be rewritten as the known Fermi-Dirac integral which in turn can be expressed using the polylogarithm function:

$$n_{s\mathrm{D}} = -N_{\mathrm{C},s} \, \mathrm{Li}_{s/2}\left(-e^{-(E_{\mathrm{C}} - E_{\mathrm{F}})/k_{\mathrm{B}} T}\right). \tag{5}$$

where $N_{\mathrm{C},s} = 2g_v \left(\frac{m^* k_{\mathrm{B}} T}{2\pi\hbar^2}\right)^{s/2}$.

For asymptotic cases of the polylogarithm:

- In the MB limit ($E_{\mathrm{C}} - E_{\mathrm{F}} \gg k_{\mathrm{B}} T$):

$$n_{s\mathrm{D}} \approx N_{\mathrm{C},s} \, \exp\left(-\frac{E_{\mathrm{C}} - E_{\mathrm{F}}}{k_{\mathrm{B}} T}\right). \tag{6}$$

- In the degenerate (low-T) limit ($E_{\mathrm{F}} \gg E_{\mathrm{C}}$):

$$n_{s\mathrm{D}} \approx \frac{N_{\mathrm{C},s}}{\Gamma(s/2 + 1)} \left(-\frac{E_{\mathrm{C}} - E_{\mathrm{F}}}{k_{\mathrm{B}} T}\right)^{s/2}. \tag{7}$$

B. Analytical Solutions for Contact Resistance

We solve Eq. (1) analytically using approximations for the derivative of the Fermi-Dirac distribution. In the MB limit, where $|df/dE| = \frac{1}{k_{\mathrm{B}} T} e^{-(E - E_{\mathrm{F}})/k_{\mathrm{B}} T}$, we find:

$$\frac{1}{R_{s\mathrm{D}}} = \frac{1}{R_{0,s}} \exp\left(-\frac{E_{\mathrm{C}} - E_{\mathrm{F}}}{k_{\mathrm{B}} T}\right), \tag{8}$$

where $R_{0,s}^{-1} = \frac{2e^2}{h} g_v \left(\frac{m^* k_{\mathrm{B}} T}{2\pi\hbar^2}\right)^{(s-1)/2}$.

Substituting Eq. (6) yields:

$$\frac{1}{R_{s\mathrm{D}}} = \frac{e^2}{h} \sqrt{\frac{2\pi\hbar^2}{m^* k_{\mathrm{B}} T}} n_{s\mathrm{D}}. \tag{9}$$

In the low-T limit, where $|df/dE| \approx \delta(E - E_{\mathrm{F}})$, the contact resistance becomes:

$$\frac{1}{R_{s\mathrm{D}}} = \frac{1}{R_{0,s} \Gamma\left(\frac{s+1}{2}\right)} \left(-\frac{E_{\mathrm{C}} - E_{\mathrm{F}}}{k_{\mathrm{B}} T}\right)^{(s-1)/2}. \tag{10}$$

Substituting the carrier density from Eq. (7), we obtain:

$$\frac{1}{R_{s\mathrm{D}}} = \frac{e^2}{h} \frac{(2g_v)^{1/s}}{\Gamma\left(\frac{s+1}{2}\right)} \left(\Gamma\left(\frac{s}{2} + 1\right) n_{s\mathrm{D}}\right)^{(s-1)/s}. \tag{11}$$

Explicit solutions for the 1D, 2D, and 3D dimensionalities in the low-T limit:

$$R_{1\mathrm{D}} = \frac{h}{2e^2} \frac{1}{g_v}, \tag{12}$$

$$R_{2\mathrm{D}} = \frac{h}{2e^2} \sqrt{\frac{\pi}{2 g_v n_{2\mathrm{D}}}}, \tag{13}$$

$$R_{3\mathrm{D}} = \frac{h}{e^2} \left(\frac{4}{3\sqrt{2\pi g_v} n_{3\mathrm{D}}}\right)^{2/3}. \tag{14}$$

C. Poisson Equation and Transport Modeling

To account for electrostatic effects in different dimensional systems, we solve the Poisson equation numerically for nanowire (3D), monolayer (2D), and bulk (1D) geometries. The electrostatic potential energy $U(x)$ is obtained by solving

$$\nabla^2 U = \frac{e^2}{\epsilon} \frac{1}{t^{3-s}} \left[N_{\mathrm{D},s} + N_{\mathrm{C},s} \, \mathrm{Li}_{s/2}\left(-\exp\left(-\frac{U - E_{\mathrm{F}}}{k_{\mathrm{B}} T}\right)\right)\right], \tag{15}$$

where ϵ is the dielectric constant, t is the thickness of the low-dimensional material, $N_{\mathrm{D},s}$ is the doping concentration, and $N_{\mathrm{C},s}$ is the effective density of states for an s-dimensional material. The potential energy is obtained by self-consistently solving for the carrier density given by the polylogarithmic form of the Fermi–Dirac integral.

We discretize the Poisson equation using a finite-difference scheme on a rectangular grid. The domain extends to $x_{\max} = 300\,\mathrm{nm}$ in the transport direction (with 0.5 nm grid spacing) and 50 nm in the transverse directions (with 0.2 nm spacing). A uniform dielectric constant of $\epsilon = 3.9\,\epsilon_0$ and an effective mass $m^* = 0.5\,m_e$ are assumed throughout. The semiconductor thickness is set to $t \approx 1\,\mathrm{nm}$, and carrier density is assumed to vanish outside the semiconductor region.

Boundary conditions are chosen as follows: a Dirichlet condition is applied at $x = 0\,\mathrm{nm}$, constituting the Schottky barrier of 0.3 eV; all other boundaries are treated using Neumann conditions. The Fermi level is fixed at $E_{\mathrm{F}} = 0\,\mathrm{eV}$.

From the computed potential profiles, we extract the electrostatic potential at the center of the semiconductor and use Eq. (1) to calculate the contact resistance. The transmission probability $T(\mathbf{k}, E)$ is evaluated using the WKB approximation:

$$T(\mathbf{k}, E) = \exp\left[-2 \int_0^{x_{\max}} dx \sqrt{\frac{2m^*}{\hbar^2}\left(E - \left[U(x) + \frac{\hbar^2 |\mathbf{k}|^2}{2m^*}\right]\right)}\right]. \tag{16}$$

This framework allows us to assess the role of electrostatics in determining contact resistance and compare it directly with the ideal quantum-limited values.

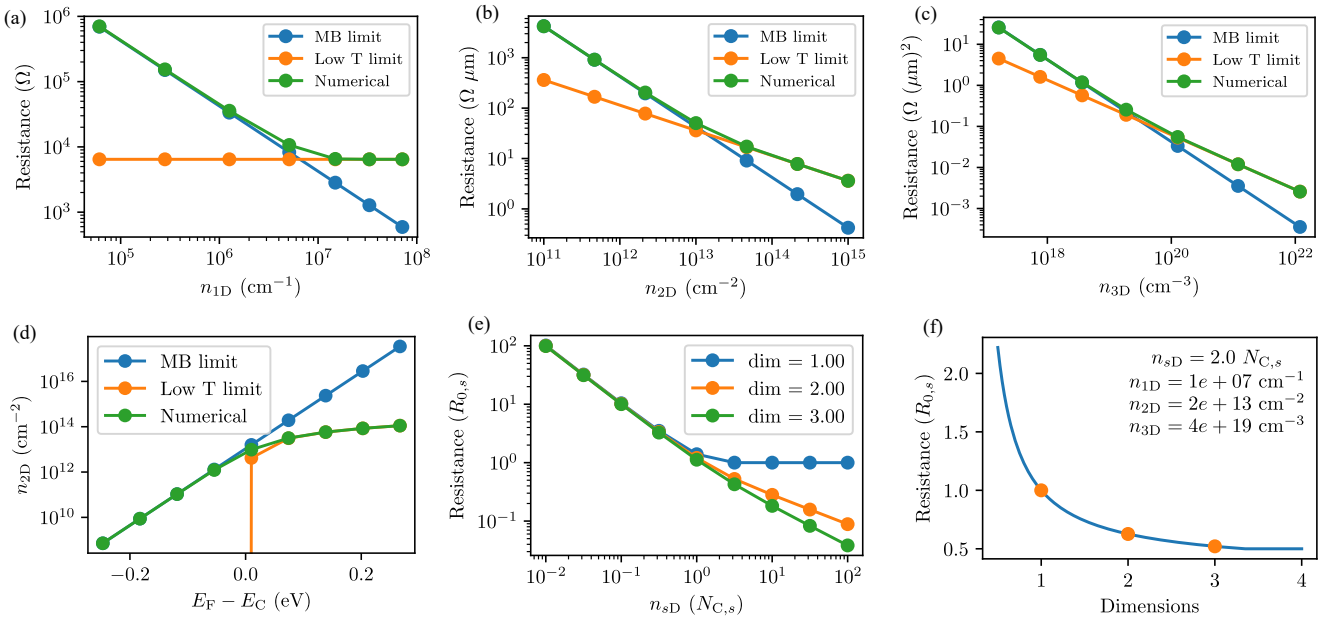

Fig. 2. Quantum limit (QL) of contact resistance as a function of carrier density in different dimensional systems. (a–c) Numerically calculated QL (green) compared with analytical approximations in the Maxwell–Boltzmann (MB) regime (blue) and the low-temperature (degenerate) regime (orange) for (a) 1D, (b) 2D, and (c) 3D semiconductors. (d) Carrier density in a 2D material as a function of conduction band minimum E_C, computed numerically and compared with MB and low-T approximations. (e) Normalized contact resistance $R_{sD}/R_{0,s}$ as a function of normalized carrier density $n_{sD}/N_{C,s}$ for different dimensions. (f) QL of contact resistance evaluated at $n_{sD} = 2N_{C,s}$ as a function of continuous dimensionality.

III. Results

Figures 2(a)–(c) present the QL of contact resistance for 1D, 2D, and 3D semiconductor systems. The results compare the numerically obtained QL by evaluating Eq.(1) with analytical expressions derived for the Maxwell–Boltzmann (MB) regime (Eq.(9)) and the degenerate (low-temperature) regime (Eq. (11)).

At low carrier densities, the MB approximation accurately describes the QL across all dimensionalities. At higher densities, where carriers become degenerate, the low-T expression becomes valid. The maximum resistance between the low-T and MB limits provides a good approximation for the true QL.

Figure 2(a) shows that in 1D systems, contact resistance approaches a fixed lower bound, given by the quantum of resistance $R = h/(2e^2 g_v)$, and cannot be reduced further regardless of carrier concentration. In contrast, Figures 2(b) and (c) demonstrate that 2D and 3D systems exhibit no such hard floor. Their QLs continue to decrease with increasing carrier density, consistent with Eqs. (13) and (14), although practical doping limits constrain how far this reduction can go.

Figure 2(d) compares the 2D carrier density as a function of conduction band minimum E_C using the numerically evaluated, full polylogarithmic expression (Eq.5) with the analytic expressions in the MB (Eq.6) and low-T limit (Eq. 7). The MB and low-T approximations agree with the numerical solution in their respective limits, deviating only near the transition region around $E_C \approx E_F \pm 2k_B T$. Similar behavior is found for 1D and 3D systems.

Figure 2(e) compares QL behavior across dimensionalities by plotting normalized contact resistance ($R_{sD}/R_{0,s}$) versus normalized carrier density ($n_{sD}/N_{C,s}$). At low carrier densities, all systems show a universal trend independent of dimensionality. In the degenerate regime, dimensionality becomes significant: 1D systems reach a hard lower limit, 2D systems exhibit higher QL values than 3D, and 3D systems achieve the lowest resistance for the same normalized carrier concentration. Most transistor designs aim for degenerately doped contacts, which leads to inherently higher QL in low-dimensional materials compared to bulk semiconductors.

Figure 2(f) plots the QL at a fixed degenerate carrier density ($n_{sD} = 2N_{C,s}$) versus continuous dimensionality s from 0.5 to 4. The contact resistance increases rapidly as dimensionality decreases, showing that miniaturization comes at the cost of higher fundamental resistance.

Figures 3(a)–(c) show numerically computed electrostatic potential energy profiles for 1D (bulk), 2D (monolayer), and 3D (nanowire) structures. All systems are simulated with doping levels chosen to yield a conduction band energy of 0.8 eV. In (b) and (c), the semiconductor boundaries are marked by red lines. Figure 3(d) shows potential profiles along the center of each structure. The depletion width increases with decreasing dimensionality due to reduced electrostatic screening in lower-dimensional systems.

Figure 3(e) presents the contact resistance as a function of doping concentration. At low doping, resistance values are comparable across dimensions, despite drastically different

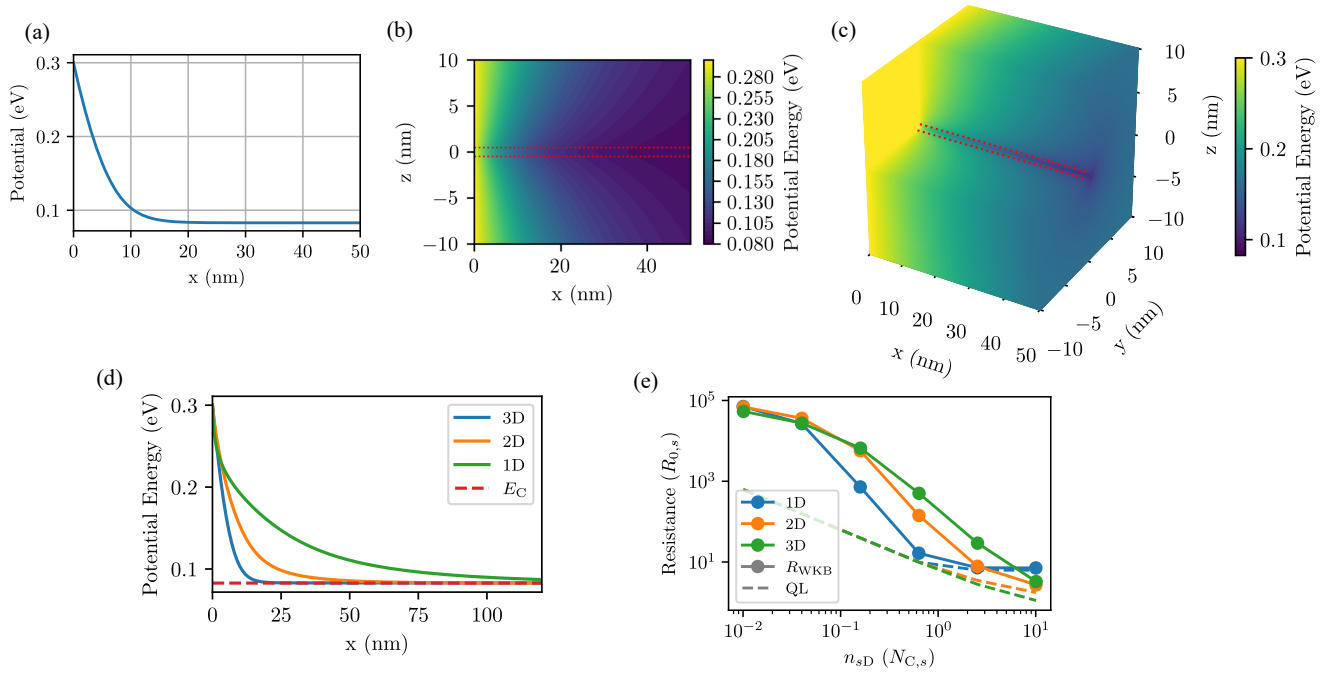

Fig. 3. Electrostatic potential energy profiles and corresponding contact resistance in 1D, 2D, and 3D semiconductor contacts. (a–c) Simulated electrostatic potential energy in bulk (1D), monolayer (2D), and nanowire (3D) geometries, respectively. In (b) and (c), red lines denote the spatial boundaries of the semiconductor. (d) Cross-sectional potential profiles extracted from the center of each structure. (e) Contact resistance as a function of doping concentration for each dimensionality.

depletion widths. As doping increases, resistance drops more steeply in 1D and 2D systems, reaching their respective QLs more quickly than in 3D, due to both their larger electrostatic sensitivity and inherently higher $R_{0,s}$. Although 3D systems eventually achieve lower absolute resistance, they require much higher carrier concentrations to do so.

IV. Conclusion

We derived analytical approximations based on the Fermi-Dirac distribution which effectively capture the QL across carrier densities, closely matching numerical results when considering MB approximation at low carrier densities and the low-T approximation at high carrier densities.

At non-degenerate carrier densities, the QL is dimension-independent, while at degenerate densities, the QL increases exponentially as dimensionality decreases. In 1D systems, resistance is fundamentally limited by the quantum of resistance and remains largely unaffected by carrier concentration, unlike in 2D and 3D systems.

Additionally, we examined transport in simple edge-contact geometries to assess the influence of electrostatics on the actual contact resistance. The depletion width at the contact interface varies with dimensionality due to differences in screening, which in turn affects the sensitivity of the contact resistance to the doping concentration. Low-dimensional materials exhibit the strongest reduction in contact resistance at moderate doping levels, as their electrostatics are more sensitive to doping changes. In contrast, bulk materials show the most effective scaling at high doping levels, where contact resistance is ultimately limited by the QL.

References

[1] R. Landauer, "Spatial variation of currents and fields due to localized scatterers in metallic conduction," *IBM Journal of Research and Development*, vol. 1, no. 3, pp. 223–231, 1957.

[2] S. Datta, *Electronic Transport in Mesoscopic Systems*, ser. Cambridge Studies in Semiconductor Physics and Microelectronic Engineering. Cambridge University Press, 1995.

[3] W. Li, X. Gong, Z. Yu, L. Ma, W. Sun, S. Gao, Ç. Köroğlu, W. Wang, L. Liu, T. Li, H. Ning, D. Fan, Y. Xu, X. Tu, T. Xu, L. Sun, W. Wang, J. Lu, Z. Ni, J. Li, X. Duan, P. Wang, Y. Nie, H. Qiu, Y. Shi, E. Pop, J. Wang, and X. Wang, "Approaching the quantum limit in two-dimensional semiconductor contacts," *Nature*, vol. 613, no. 7943, pp. 274–279, Jan 2023. [Online]. Available: https://doi.org/10.1038/s41586-022-05431-4

[4] P.-C. Shen, C. Su, Y. Lin, A.-S. Chou, C.-C. Cheng, J.-H. Park, M.-H. Chiu, A.-Y. Lu, H.-L. Tang, M. M. Tavakoli, G. Pitner, X. Ji, Z. Cai, N. Mao, J. Wang, V. Tung, J. Li, J. Bokor, A. Zettl, C.-I. Wu, T. Palacios, L.-J. Li, and J. Kong, "Ultralow contact resistance between semimetal and monolayer semiconductors," *Nature*, vol. 593, no. 7858, pp. 211–217, May 2021. [Online]. Available: https://doi.org/10.1038/s41586-021-03472-9

[5] A. Mondal, C. Biswas, S. Park, W. Cha, S.-H. Kang, M. Yoon, S. H. Choi, K. K. Kim, and Y. H. Lee, "Low ohmic contact resistance and high on/off ratio in transition metal dichalcogenides field-effect transistors via residue-free transfer," *Nature Nanotechnology*, vol. 19, no. 1, pp. 34–43, Jan 2024. [Online]. Available: https://doi.org/10.1038/s41565-023-01497-x

[6] D. Akinwande, C. Biswas, and D. Jena, "The quantum limits of contact resistance and ballistic transport in 2d transistors," *Nature Electronics*, vol. 8, no. 2, pp. 96–98, Feb 2025. [Online]. Available: https://doi.org/10.1038/s41928-024-01335-5